Molecular Neurobiology (2025) 62:8065–8083
https://doi.org/10.1007/s12035-025-04735-6

RESEARCH

# IGF1R/ARRB1 Mediated Regulation of ERK and cAMP Pathways in Response to Aβ Unfolds Novel Therapeutic Avenue in Alzheimer's Disease

**Priyanka Sengupta[1,2] · Debashis Mukhopadhyay[1,2]**

Received: 17 July 2024 / Accepted: 31 January 2025 / Published online: 19 February 2025


**Abstract**

IGF1R/INSR signaling is crucial for understanding Alzheimer's disease (AD) and may aid in the development of potent therapeutic strategies. This study investigated the expression and activity of these receptors and their potential to form functional hybrids in response to amyloid beta (Aβ). IGF1R, INSR, and ARRB1 were found to be upregulated in AD. The propensity for functional hybrid formation was also greater in the presence of Aβ. The association of IGF1R with ARRB1 reached a maximum at 60 min of Aβ treatment, which coincided with increased pERK activity at approximately the same time, indicating the importance of this association in pERK regulation. Knocking down IGF1R, INSR, and ARRB1 independently reduced cAMP, whereas overexpressing IGF1R significantly increased cAMP. Knocking down ARRB1 in IGF1R-overexpressing cells led to a reduction in cAMP, indicating that the interaction of ARRB1 and IGF1R possibly contributes to cAMP dysregulation. Since cAMP plays a crucial role in cognition and memory, alterations in cAMP after receptor hybridization could be significant in AD. Additionally, we noted hyperactivation of MAPK, which is associated with aberrant cellular activity, transcriptional control, and stress pathways. This finding highlights the importance of IGF1R and INSR dysregulation, which plays a major role in addition to conventional RTK signaling through multiple pathways. Here, we focused on the ARRB1 and IGF1R interaction and showed that picropodophyllin (PPP), an IGF1R-specific inhibitor, blocks this interaction and alters the ERK and cAMP status under disease conditions. Cell viability studies further revealed that the PPP substantially improved cell viability in the presence of Aβ. This highlights the role of the PPP in regulating these cascades and opens the arena for further therapeutic development for AD.

✉ Debashis Mukhopadhyay
debashis.mukhopadhyay@saha.ac.in

[1] Biophysical Sciences Group, 1/AF, Biddhanagar, Saha Institute of Nuclear Physics, Kolkata 700064, India

[2] Homi Bhabha National Institute, Anushaktinagar, Mumbai 400094, India

**Graphical Abstract**

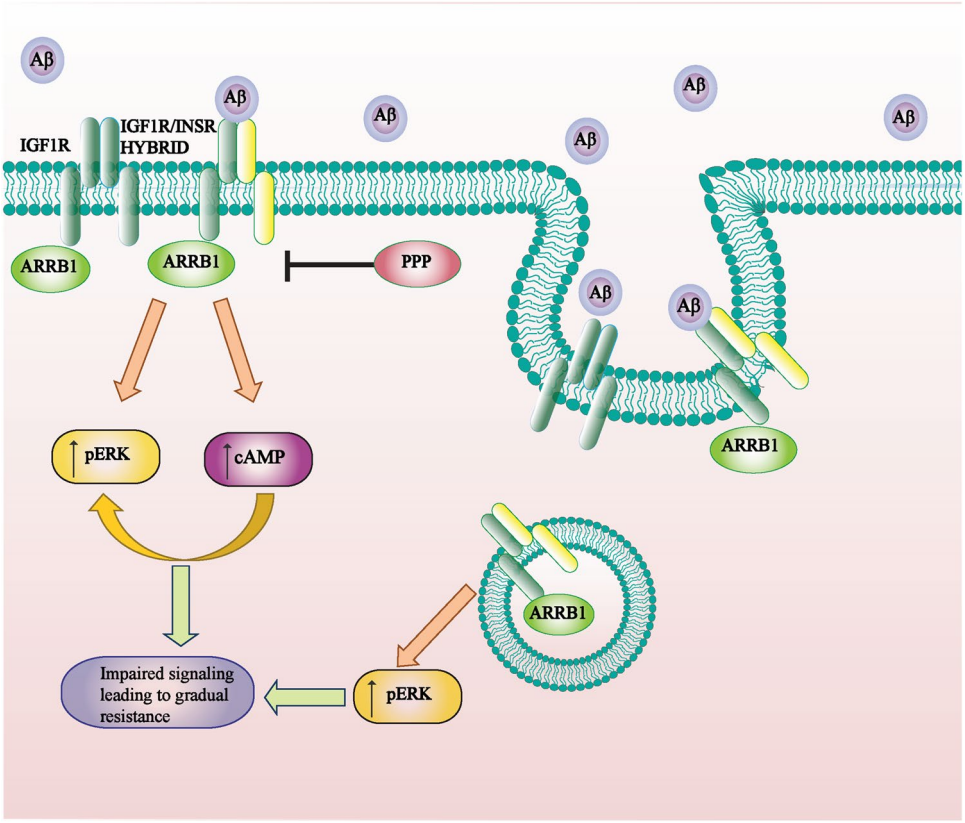


**Keywords** Alzheimer's disease · IGF1R · ARRB1 · cAMP · Degenerative signaling

**Abbreviations**

| | |
|---|---|
| Aβ | Amyloid beta |
| AD | Alzheimer's disease |
| IGF1R | Insulin-like growth factor 1 receptor |
| INSR | Insulin receptor |
| ARRB1 | Beta-arrestin 1 |
| PPP | Picropodophyllin |
| BMS | BMS 536924 |
| Lns | Linsitinib |

## Introduction

Alzheimer's disease (AD) is the most common form of dementia [1] and involves neurodegeneration, neuroinflammation, and neuronal death due to unknown causes [2, 3]. The insulin pathway has long been implicated in different aspects of this disease, including metabolic, signaling, and systemic resistance paradigms [4, 5]. This has led to an interest in the insulin receptor family (IRF), which primarily includes insulin receptor (INSR), insulin-like growth factor receptor (IGFR), and insulin-related receptor (IRR) [6, 7]. INSR has been extensively studied in AD [8–10] for a long time, and its ligand, insulin, is being used for intranasal therapy for treating AD patients [11]. However, owing to the complexity of the receptor and its subsequent regulatory pathways, insulin growth factor 1 (IGF1) signaling is poorly understood [12], and several gaps in understanding this mechanism exist [5, 13]. The extracellular domains of the two receptors, IGF1R and INSR, can bind to the ligands, insulin, IGF1, and IGF2 interchangeably; however, their binding affinities differ. Their ectodomains are highly similar [14], whereas they differ in terms of their endodomain (only 44% homology at the C-terminus), which allows INSR to exhibit metabolic effects and IGF1R to regulate proliferative events [15]. IGF1R has a wide variety of binding sites for several cytosolic proteins, including canonical binding sites for IRS1, RACK1, Vav3, 14.3.3, Grb10, Shp2, PI3K, IRS1-4, Shc, Crk2, CrkL, p125FAK, and, importantly, β-arrestin 1 (ARRB1) binding sites (S1248 and S1291 residues in the IGF1R endodomain) in the cytoplasmic tail [16]. This further adds to the complexity of its downstream

signaling pathway. β-arrestins (ARRBs), as signaling partners in GPCR signaling, are currently an evolving paradigm [17], but less is known about the mechanisms involved in RTK signaling. Studies focusing on holistic transcriptomic analysis and signaling have shown that abrogation of IGF1R leads to improvements in memory and cognitive abilities in patients with AD [13, 18], which makes IGF1R a crucial target for understanding AD pathology. Structural studies of these receptors have investigated functional hybrids (HybRs), viz., IGF1R/InsR hybrids [19, 20], and characterized the interfacing domains. These hybrids are extremely important for understanding their functional roles, as they can potentially interact with amyloid beta (Aβ) and exploit the ERK, Akt, and β-arrestin-mediated signaling pathways in response to Aβ plaques, which are hallmarks of AD. HybR has been studied in breast cancer, and HybR functions differently from holoreceptors [21], where such a hybrid has a higher affinity for binding to IGF1 than insulin [19, 20]. However, to date, no studies have been conducted on the existence or functional involvement of these HybRs in a neurodegenerative scenario.

There are two conventionally studied pathways for the receptors IGF1R and INSR: the MAPK pathway and the PI3K/Akt pathway. Upon ligand binding, the cytoplasmic tails of RTKs or GPCRs are generally phosphorylated, and downstream adaptor molecules bind to the activated phosphorylated tail at different sites, escalating different signaling cascades [17, 22]. Previous reports have shown a decrease in PI3K/Akt signaling in AD, which is ameliorated by treatment with different agents [23]. However, MAP kinase pathways, including the ERK, JNK, and p38/SAPK pathways, are reportedly altered in AD, although discrepancies exist [24–26]. The ERK pathway is classically regulated by extracellular signals or ligands, whereas JNK and p38 are regulated by stress, cytokines, and GPCR agonists [27]. Stimulation of INSR/IGF1R leads to the phosphorylation of ERK 1/2 [5]; hence, this study focused closely on this set of MAPK signaling pathways. Furthermore, in AD, all MAPK signaling pathways are activated in vulnerable neurons, suggesting that this alteration is a probable early disease marker that is sustained for long periods during the progression of the disease [24, 26, 28–30].

To this end, the focus of our work has remained on exploring the signaling cascade that begins with the introduction of Aβ and the role of IGF1R/INSR in mediating downstream pathways. The binding of β-arrestin adds a new paradigm to this cascade, in which the GPCR pathway potentially overlaps with endosomal signaling and cAMP triggers. However, the penultimate fate of the receptor remains to be understood. There are three distinct possibilities for this process: receptor recycling to the membrane, degradation [31], and nuclear shuttling [32–37]. We investigated these possibilities to decipher the consequences of hyperphosphorylated ERK signaling, which is imperative since the Aβ plaque burden is ever increasing during disease progression, correlating it with disease stage [38, 39]. Nuclear shuttling of these receptors has been previously shown in different cell lines [32] but in response to ligand stimulation or cancer. For the first time, we attempted to understand whether there is any bias in the shuttling of these receptors in AD.

## Materials and Methods

### Bioinformatic Analysis

The 4 pertinent molecular interactions in focus here, INSR, IGF1R, ARRB1, and ARRB2, were submitted to Metascape [40]. Clustering was performed via the Gene Ontology (GO) database [41] and Kyoto Encyclopedia of Genes and Genomes (KEGG) database [42]. For cluster formation on the basis of functional relevance in pathways, the cutoff was a 0.3 similarity threshold. Furthermore, the mature complex identification algorithm (MCODE) [43], which automatically extracts protein complexes from networks, was used. Metascape uses the data from DisGeNET (database for gene–disease associations) [42] and correlates them through a hypergeometric test and the Benjamini−Hochberg *p*-value correction algorithm, which shows the correlation of selected genes with particular disease conditions.

### Cell Culture and Transfection

SHSY5Y cells used for the experiments were obtained from NCCS, Pune, India, and were routinely cultured in DMEM-F12 (Gibco) supplemented with 10% heat-inactivated FBS (Gibco) and 1% Penstrep cocktail (v/v). The N2A cells used for the supplementary experiments were obtained from NCCS, Pune, India, and were routinely cultured in DMEM (Gibco) supplemented with 10% heat-inactivated FBS (Gibco) and 1% Penstrep cocktail (v/v). These cells were maintained at 37 °C in 5% $CO_2$. Transfections were carried out at 50–60% confluency. One microgram of plasmid DNA construct (for 35 mm plates) was incubated with 5 µl of Lipofectamine 2000 (Invitrogen) in 250 µl of serum-free media for transfection. IGF1R (HG10164-ACG) and the INSR spark clone (HG11081-ACG) were purchased from Sino Biological, and normalization of the transfection was conducted by using the GFPSpark Control vector (Cat: CV026). Arrb1-RFP was a kind gift from Dr. Robert Lefkowitz (Addgene plasmid #35401) [44], and RnBarr2-mCherry (Addgene plasmid #137794) was a kind gift from Dr. Dorus Gadella [45]. Knockdown experiments were conducted using Mission esiRNAs against IGF1R (EHU028861), Thermo Fisher siRNAs against ARRB1 (4427037, assay ID: s1622), Thermo Fisher siRNAs against

ARRB2 (4427037, assay ID: s1625), and Thermo Fisher siRNAs against INSR (AM16708, assay ID: 103297).

## Working Cell Models of AD

Only GFP constructs and constructs containing the amyloid precursor protein intracellular domain (AICD) with GFP were used for model development [12, 41, 46, 47] along with Aβ. The constructs were transfected with Lipofectamine 2000 (Invitrogen), and the efficiency of transfection was checked via a confocal microscope. After the stock solution was incubated with 2 mM $A\beta_{1-42}$ peptide (Sigma−Aldrich) at 37 °C for 30 min, the oligomers were then introduced into the media at a concentration of 0.5 µM after 3 h. Several studies [48–52] have shown empirically that it takes approximately 10 min at minimum for half the amount of Aβ(1–42) used by us to form oligomers and aggregates. However, since 0.5 µM has been extensively used and validated as a functional model, it was specifically employed here for model development. Samples were collected 48 h posttreatment. For AD model development, the above procedure was followed. For all other experiments, the $A\beta_{1-42}$ peptide was prepared in the same way, and the same concentration was introduced into the media for the mentioned durations.

## RNA Isolation from Cells, cDNA Preparation, and Quantitative Real-Time PCR

Total RNA was extracted from cultured SHSY5Y cells via TRIzol (Invitrogen, USA) according to the manufacturer's protocol. Two micrograms of total RNA was treated with DNase (Sigma) to prepare cDNA via random hexamer primers, dNTPs, and reverse transcriptase enzyme (Fermentas). Quantitative real-time PCR (qRT−PCR) was conducted via SyBr Green (Promega) in a real-time PCR system 7500 (Applied Biosystems) and/or Quant Studio 3 (Applied Biosystems). For each sample, GAPDH was used as an internal control to normalize the data.

## Gene-Specific Primers

The primers used for IGF1R were 5′ACGAGTGGAGAA ATCTGCGG3′ (forward) and 5′ACTCGGTAATGACCG TGAGC3′ (reverse). The primers used for INSR were 5′CGGAACCCACCTATTTCTACG3′ (forward) and 5′CCA TCTGGCTGCCTCTTTCT3′ (reverse). For ARRB1, 5′CAA AGGGACCCGAGTGTTCA3′ (forward) and 5′CAGGAC CACACCATCCACAG3′ (reverse), and for ARRB2, 5′TGT GTCTGGGGTGGGGATAC3′ and 5′AGCCGCACAGAG TTCCTTTTT3′ were used for qRT−PCR. The housekeeping primers used for GAPDH were 5′GACAGTCAGCCGCAT CTTCT3′ (forward) and 5′GCGCCCAATACGACCAAA TC3′ (reverse).

## Western Blot Analysis

After transfection, the cell pellets were washed in PBS (1×) and lysed in lysis buffer (Invitrogen, FNN0011) supplemented with 1 mM PMSF and a protease inhibitor cocktail. After 30 min, the samples were spun at 13,000 RCF for 15 min. The supernatants were collected and quantified via the Bradford assay. Equal amounts of lysate were separated via SDS−PAGE, transferred to PVDF membranes (Millipore), and blocked with 5% skim milk in TBST. An Abcam antibody (ab182408) (EPR19322) against IGF1R was used at a 1:1000 dilution in TBST for probing overnight. The same process was followed for Akt (ab235958). CST antibodies against ARRB1 (mAb #12697), pAKT (#9271), and SCB (sc13140) were used at a 1:500 dilution, and CST antibodies against pERK (#9101) and ERK (#9102) were used at a 1:1000 dilution. A secondary antibody from Invitrogen (31210) was used at a 1:3000 dilution, and the blots were developed with an enhanced chemiluminescence (ECL) kit (SuperSignal West Pico Substrate; Pierce). Blots were quantified via an Azure Imaging 200 system and Azurespot Pro Analysis software. Band intensities were normalized to the loading control.

## Immunoprecipitation

Immunoprecipitation was performed as described by Slaaby [53]. Aβ was added to the media for 48 h, after which the samples were harvested from 100 mm dishes in 100 µl of lysis buffer (Thermo Fisher Scientific) supplemented with sodium orthovanadate and Tween 20. For immunoprecipitation, 30 µl of protein A/G-agarose (Invitrogen) was added to 300 µl of buffer containing HEPES (pH 7.8), NaCl, $MgSO_4$, Tween-20, and 1 µg of the antibody for 3 h at 4 °C, followed by brief centrifugation at 1800×g. The precipitates were washed three times in wash buffer containing PBS, Tween-20, $Na_3VO_4$, 1 mM AEBSF, and 1 mg/ml p-nitrophenyl phosphate. These precipitates were then heated in SDS sample buffer for 15 min before being subjected to SDS−PAGE. To develop the blots, a Veriblot (ab131366) was used. To check for efficiency and IP outcome, two different gels were run, as both proteins were probed with the same/close molecular weights.

## Cyclic AMP Assay

The cyclic AMP assay was performed according to the manufacturer's protocol (Promega Cat. No. V1501). In brief, cells were seeded equally on poly-L-lysine-coated 96-well plates after counting on a hemocytometer, and media was added to allow for adherence and growth overnight. The respective inhibitors and blockers, siRNAs, and/or clones were introduced into induction buffer containing serum-free

F12/DMEM supplemented with 500 µM IBMX (#I5879, Sigma) and 100 µM Ro 20–1724 (#557502, Sigma). PPP (picropodophyllin), purchased from Sigma (#407247); BMS 536924 (BMS), purchased from Tocris (#4774); and Linsitinib (Lns), purchased from MedchemExpress (#HY10191), were resuspended in DMSO. PPP, Lns, and BMS were added at a concentration of 1 µM [54–56]. Recombinant human IGF-I was purchased from PreproTech (100–11), and insulin (#I9278) was obtained from Sigma−Aldrich. IGF1 was resuspended in BSA (#A8806) from Sigma and added at a final concentration of 10 nM [57]. Insulin substocks were made in media and added at a final concentration of 10 nM [41]. The inhibitor, blocker, and siRNA experiments were conducted for 24 h in induction buffer, and cAMP Glo lysis buffer and detection solution containing PKA and kinase Glo were subsequently added and incubated for 15, 20, and 10 min, respectively. Luminescence was measured via a BioTek Synergy HTX multimode reader. The data were analyzed via a standard curve generated by a provided material in kit (cAMP), and regression analysis was performed to correlate the luminescence output with the cAMP concentration to calculate the accumulation in individual sample sets. These experiments were performed in biological triplicates.

### Confocal Microscopy

Images were obtained on a Nikon NSIM microscope. The Ezcolocalization plugin [58] was used to determine the correlation coefficient. Plot intensity profiles were generated via the ImageJ "Plot profile" plugin [59]. For the ICC-based experiment, the cells were treated with Aβ for specific time periods, and then ICC was performed as described by Saha et al. [60]. The samples were stained with an antibody against IGF1R, and images were acquired on the abovementioned microscope with a 100× objective and 2× zoom using a resonant scanner and/or a Galvano scanner. The same settings were used for each individual experiment. The calculations and graphing were performed on Origin Pro 2024 (OriginLab Corporation, Northampton, MA, USA).

### Cell Viability Assay

CellTiter Glo Luminescent Viability Assay (Promega, G7570) was performed to analyze the viability of the cells after treatment with drugs and ligands to determine the impact of prolonged signaling through the abovementioned pathways. The assay was performed according to the manufacturer's protocol. In brief, cells were seeded equally into 96-well plates after counting on a hemocytometer, and media was added to allow for adherence and growth overnight. The respective inhibitors and blockers, siRNAs, and/or clones were introduced into serum-free F12/DMEM cells for up to 48 h, which were then lysed with the provided reagents. The plates were allowed to incubate while shaking for 2 min, after which signal stabilization was allowed for 15 min. The output was subsequently measured on a BioTek Synergy HTX multimode reader. The raw luminescence values provided an understanding of ATP, indicating a viable cell population. A titration of signal output against a specific number of cells ranging from $10\times10^3$ to $60\times10^3$ was performed by using the same kit to determine the number of cells per treatment thereafter.

### Statistical Analysis

For each experimental set, the statistical significance was determined through Student's unpaired *t*-test via Origin Pro 2024. For comparisons of more than 2 samples, ANOVA was applied via the aforementioned software.

## Results

### Functional Clusters of INSR, IGF1R, ARRB1, and ARRB2 Regulate AD-Implicated Pathways

The involvement of β-arrestin 1 (ARRB1) in Alzheimer's disease is poorly understood but crucial. We performed a Metascape analysis to understand the interactions among INSR, IGF1R, ARRB1, and ARRB2. All 4 proteins clustered into four distinct pathways according to their respective known functions (Fig. 1 A.i). ARRB1, ARRB2, and INSR are involved in "receptor internalization," and ARRB1, ARRB2, and IGF1R were found to cluster under "endocytosis" (Fig. 1 A.ii). ARRB2, INSR, and IGF1R control the "response to growth factor," whereas all 4 play a role in the "MAP kinase pathway" (Fig. 1 A.ii). All four players are involved in the MAPK pathway, with *p*-values of clusters in the range of $10^{-6}$–$10^{-8}$, on the basis of GO and KEGG pathway analyses (Supplementary S1). MCODE analysis revealed that all 4 players could cohesively form a functional PPI network (Fig. 1B). Furthermore, DisGeNet analysis revealed that the 4 mentioned proteins are associated with late-onset Alzheimer's disease, with a log *p*-value of − 5.1, which shows high confidence in the association of these proteins in this disease scenario (Fig. 1C).

### The Expression of IGF1R/INSR, ARRB1, and ARRB2 Is Altered Under AD-Like Conditions

We thus aimed to understand the biological milieu of the AD working cell model by determining the protein and mRNA expression levels of the relevant genes ARRB1, ARRB2, INSR, and IGF1R. The expression of IGF1R was significantly upregulated. At the mRNA level, it significantly increased by 4.82-fold, and the relative activity of IGF1R

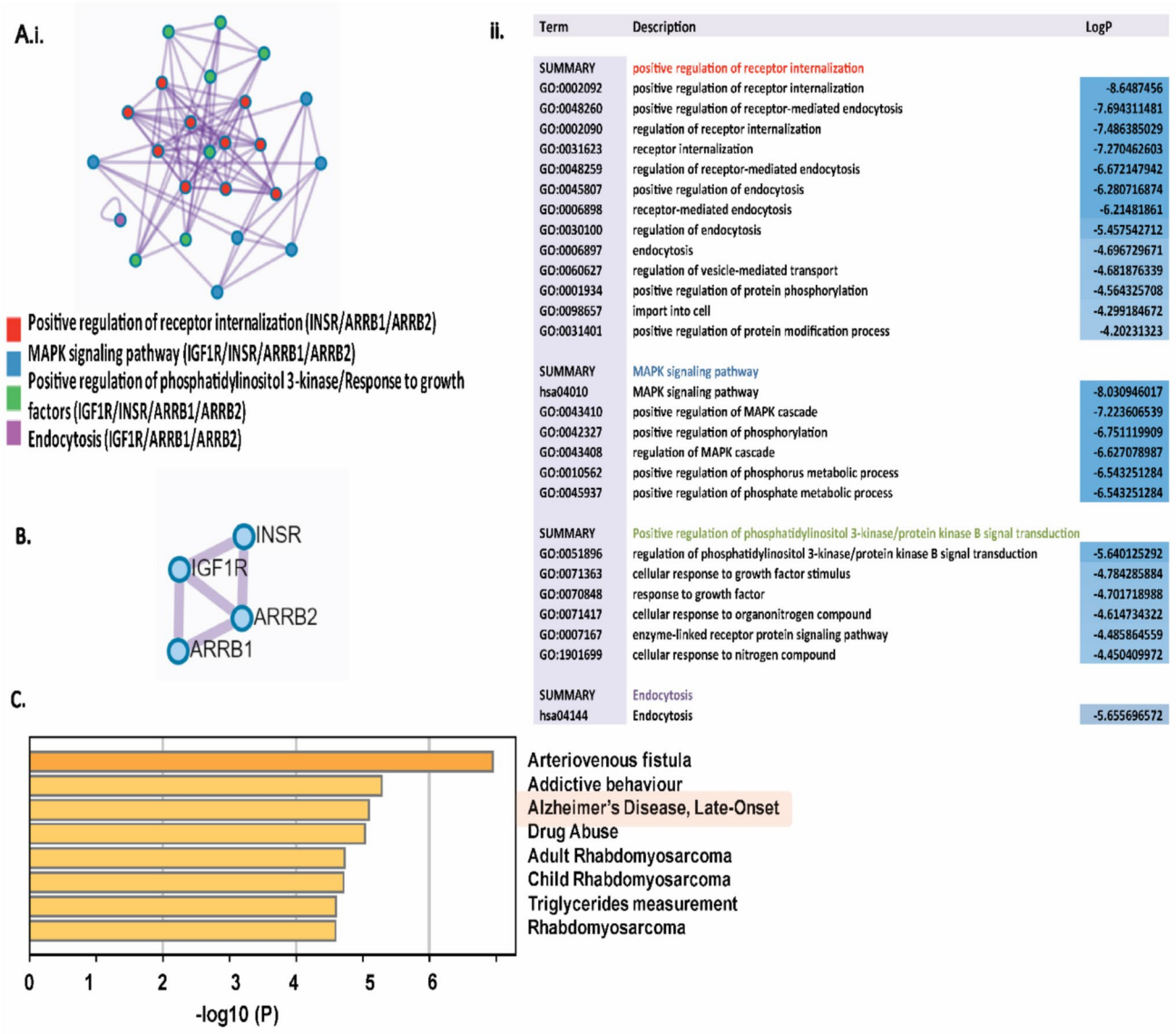


**Fig. 1** **A.i** Gene enrichment and clusters formed by INSR, IGF1R, ARRB1, and ARRB2, color-coded by their biological functions. **A.ii** shows the details of the corresponding nodes in each cluster and the confidence in the data in terms of *p*-values. **B** The MCODE results show that the four proteins form a PPI due to shared pathways. **C** Illustration of the DisGeNET-associated data that display the top clusters of diseases where the gene set is involved. Third, in the context of Alzheimer's disease, the context of this study illustrates the importance of understanding this PPI in the disease context

(pIGF1R/IGF1R ratio) increased by 1.3-fold in the AD-like scenario (Fig. 2 A.i–iii). INSR expression increased 2.3-fold at the mRNA level and 1.36-fold at the protein level (Fig. 2 B.i–iii). The significant upregulation of these genes indicated that INSR was overexpressed in AD patients. The level of phosphorylated INSR could not be calculated separately because of the homology of the β-chains of INSR and IGF1R, leading to nonspecific binding. The expression of ARRB1/2 was also altered in the study model. ARRB1 was significantly upregulated 3.3-fold at both the mRNA and protein levels (Fig. 2 Ci–iii). ARRB2 was downregulated at the protein level (Fig. 2 D.ii–iii); however, changes at the mRNA level (Fig. 2 D.i) were insignificant. Additionally, collated data from large-scale datasets generated via transcriptomic, proteomic, and biochemical analyses of mouse and/or human samples were analyzed (Table S1: Supplementary material S2), which corroborated the findings and revealed that IGF1R, INSR, and ARRB1 are upregulated not only in AD transgenic mouse models but also in human patient CSF and brain samples [8, 61–68].

Furthermore, the AD cell model is composed of two components, Aβ and AICD. Thus, to understand whether the

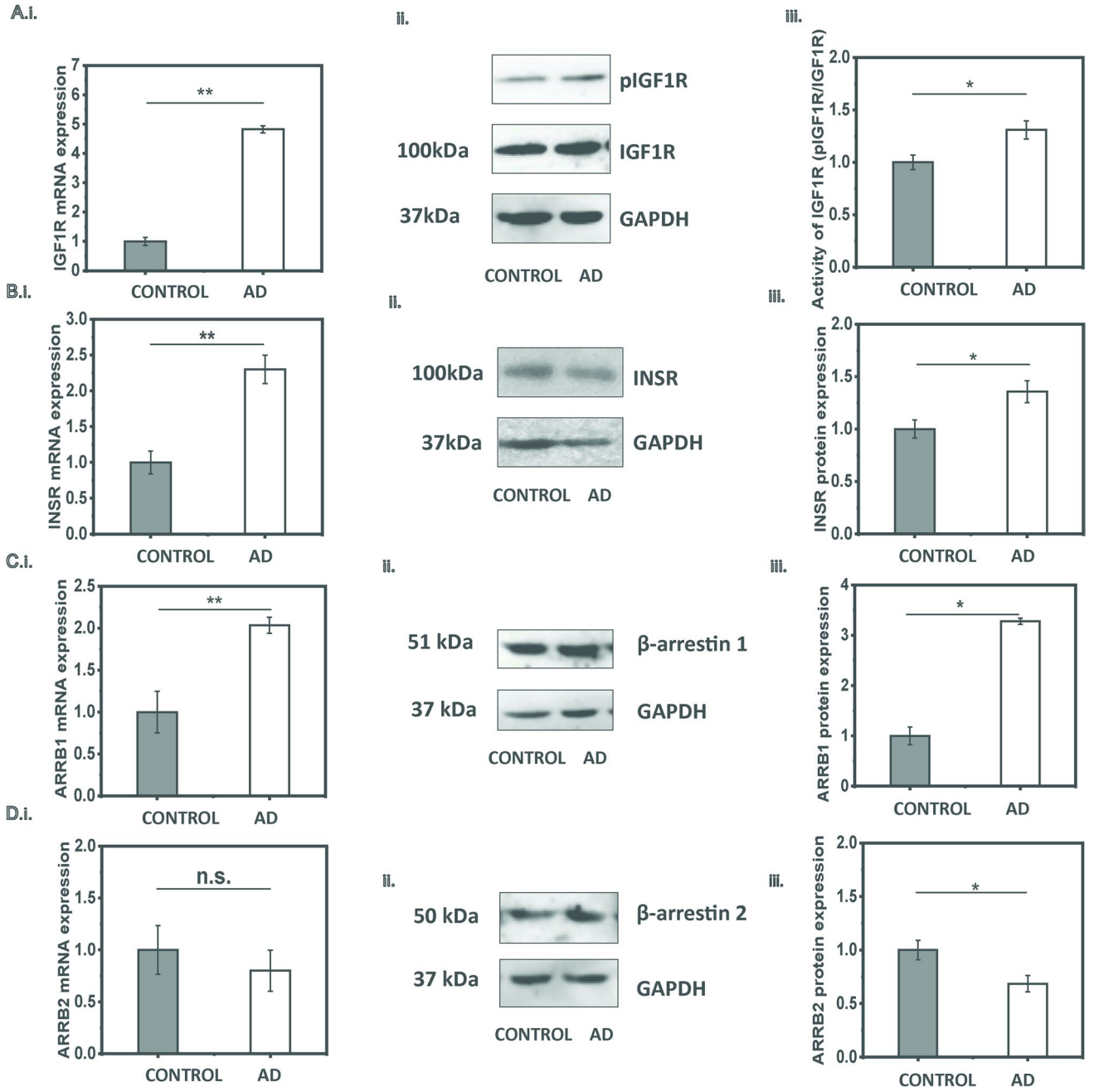


**Fig. 2** **A.i** Shows the mRNA levels of IGF1R, whereas **A.ii** Depicts the protein expression of IGF1R and its phosphorylated form. **A.iii** The activity of the receptor was obtained by normalizing the elevated activity to the elevated expression (p-IGF1R/IGF1R). **B.i** Indicates INSR mRNA expression, whereas **B.ii** and **B.iii** exhibited elevated protein expression. **C.i** Changes in β-arrestin1 (ARRB1) mRNA are shown, and **C.ii** and **iii** Changes in protein levels. **D.i** Shows that ARRB2 mRNA changes are insignificant in AD. **D.ii** Illustrates ARRB2 protein expression; **iii** Graphical representation of the changes observed for ARRB2. mRNA experiments were performed with $n=6$ samples, and protein experiments were performed with $n=3$ samples (error bars indicate ± SEMs, and the significance between pairs was calculated via Student's *t*-test and represented by stars ($*p<0.05$; $**p<0.01$))

results observed here are due to the combined impact of Aβ individually, INSR, IGF1R, and ARRB1 were further investigated at the mRNA and protein levels (Figs. S2 and S3 in Supplementary material S3). All three genes were transcriptionally upregulated (Fig. S2. A-C in Supplementary material S3), and INSR and IGF1R are translationally upregulated in the presence of Aβ (Fig. S2. D-E in Supplementary material S3). In contrast, in the presence of Aβ, GFP, AICD, or DMSO, INSR and IGF1R were upregulated at both the mRNA and protein levels (Fig. S3. A-F); however, ARRB1

appears to be more tightly regulated and is significantly dysregulated at the mRNA and protein levels only when both components are present. Independently, ARRB1 can be dysregulated by Aβ but to a lesser extent.

## IGF1R/INSR Hybrid Receptors (HybRs) Are Formed in AD-Like Conditions

As the expression of both receptors increases significantly and previous studies have reported that IGF1R can form heterodimers with INSR, it is imperative to understand whether these hybrids can form more in AD-like scenarios. They form naturally in neuroblastoma cells, N2A (mouse neuroblastoma), and SH-SY5Y (human neuroblastoma) (Supplementary material S3, Fig. S1), but the status of such dimers (HybR) has never been shown in AD. Understanding these dimers is characteristically important since INSR competes with Aβ and insulin, and such a hybrid would facilitate increased IGF1R activity. Hybrid receptor (HybR) ratios were determined by immunoprecipitating IGF1R and measuring INSR levels in the presence of Aβ (Fig. 3A). It was assumed that pIGF1R would pull down functional pINSR since RTKs generally crossphosphorylate their cytosolic domains; thus, p-IGF1R was used as bait for another set of Co-IP experiments. The percent change in immunoprecipitated INSR under disease conditions was compared with that in control cells, as shown in Fig. 2B, and a 223% greater abundance of such hybrids was detected in AD samples (Fig. 3C), whereas for phosphorylated HybR, a 311% increase was detected (Fig. 2D). The loaded samples had a 3.11-fold greater abundance of active hybrid receptors, further indicating that Aβ mediated the phosphorylation of these hybrid receptors.

## ARRB1 Is Recruited by IGF1R When Triggered by Aβ

Downstream signaling of such a hybrid could be mediated by any adaptor; however, here, we focused on β-arrestins specifically. The binding of arrestin in the presence of Aβ to IGF1R has not been previously investigated; therefore, we employed confocal microscopy in the absence of serum or any ligands with 2 mM Aβ to assess the recruitment of ARRB1 to activated IGF1R in response to Aβ. When cells were cotransfected with ARRB1 and IGF1R, increased concentrations and transfection efficiencies led to cell death and reduced viability in general; thus, the DNA load had to be

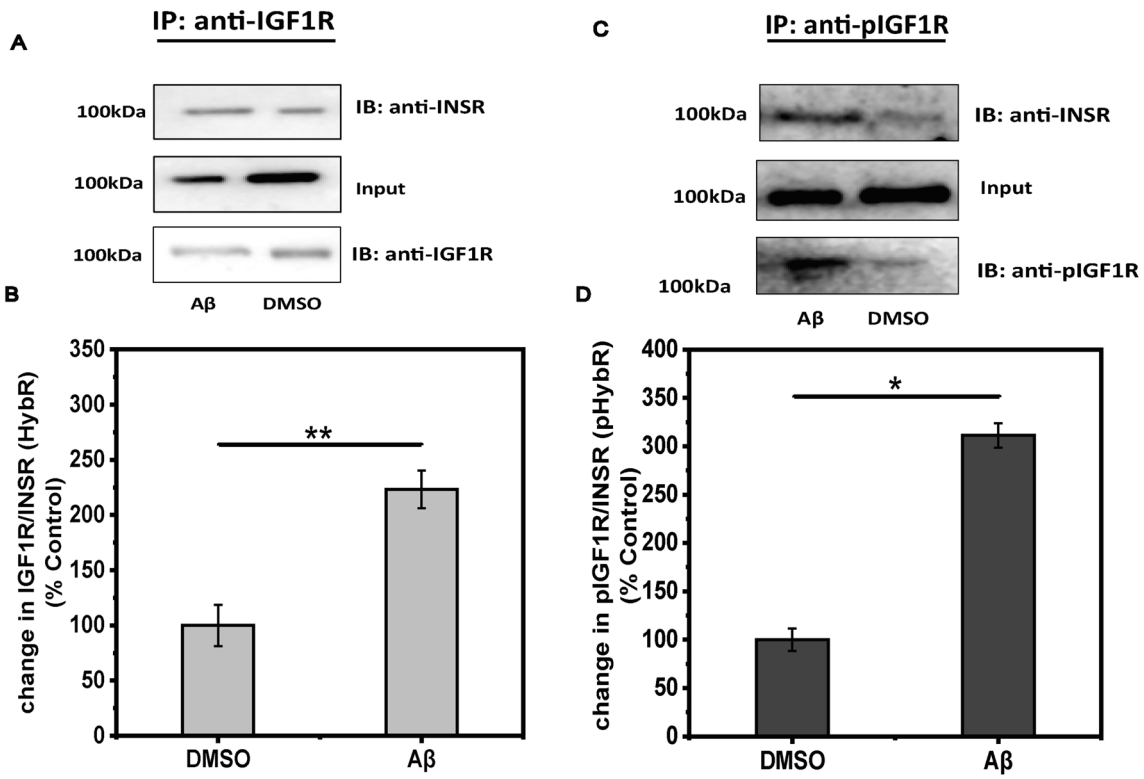


**Fig. 3** **A** IGF1R was used as bait, and the precipitated INSR is represented against the input. **B** Increased formation of the IGF1R-INSR hybrid receptor (HybR) in the presence of Aβ. Precipitated receptors were normalized with equally loaded inputs, and relative changes in control (DMSO)-versus Aβ-treated samples were calculated. **C** Illustration of the phosphorylation status of HybR. **D** Relative change in p-HybR abundance. Veriblot was used to develop the western blots. Error bars indicate ± SEMs, and the significance between pairs was calculated by Student's *t*-test and represented by asterisks (*$p < 0.05$; **$p < 0.01$)

maintained at an optimum level (0.75 µg of plasmid DNA), which allowed for visualization and cell survival after 24 h. Twenty-four hours posttransfection, the cells were treated with Aβ and fixed for 30 min (Fig. 4B), 60 min (Fig. 4C), 120 min (Fig. 4D), or 240 min (Fig. 4E) or left untreated for 0 min (Fig. 4A). Imaging experiments revealed that recruitment occurred most often in response to this stimulation at 1 h, as shown by the plot profile (Fig. 4H), with a significant PCC of 0.35 ± 0.02 SEM (Fig. 4K). The PCCs were calculated, and intensity versus distance plots for understanding the overlaps in the signals were generated with FIJI plugins (Fig. 4F–J). These responses, i.e., the recruitment of ARRB1 and membrane localization, as shown in Fig. 4C, could be due to the hybrid formation or through the formation of homodimers of IGF1R (Fig. 4L); however, these findings illustrated that Aβ acted as a trigger for the recruitment of ARRB1 to IGF1R.

The formation of punctate structures in response to Aβ might indicate vesicle formation. However, whether they functionally impact signaling needs to be verified.

## Activation of pERK Signaling in the Presence of Aβ Is Time-Dependent and Relies on the Interaction Between IGF1R and ARRB1

ARRB1 binding to IGF1R might disrupt degradation and facilitate ERK signaling in response to IGF1. To determine whether this pathway is triggered by Aβ, we analyzed ERK activity (pERK/ERK) in cells treated with Aβ for 240 min. A sharp increase in pERK activity was observed at 60 min in response to Aβ, after which the signal gradually tapered (Fig. 5A, D). At 30 min, pERK activity increased 1.29-fold and peaked at 60 min (13.4-fold). After 120 min, the average pERK activity decreased 1.17-fold; after 240 min, it started to increase 1.48-fold. To further validate whether IGF1R phosphorylation contributed to the increase in ERK signaling, the PPP (an IGF1R-specific inhibitor) was added to the cells before stimulation with Aβ (Fig. 5B, D). This led to a 3.25-fold increase at the 60-min time point. Another important factor in this context was the activity of HybR. To determine whether the hybrids contributed to this cascade, the cells were treated with BMS (an inhibitor of both IGF1R and INSR signaling) prior to stimulation with Aβ, which dramatically lowered pERK (Fig. 5C, D). These results clearly showed that blocking the phosphorylation of IGF1R and/or that of IGF1R/INSR hindered the downstream phosphorylation of ERK, as the PPP selectively blocked IGF1R, whereas BMS blocked both IGF1R and INSR activities. However, the hyperactivation of ERK might also be due to canonical RTK signaling or signaling triggered by ARRB1 binding. Thus, the pERK status at 60 min was verified in IGF1R-overexpressing SHSY5Y cells in which ARRB1 was knocked down with negative control siRNA (NC Si) overexpressing IGF1R in the presence of Aβ (Fig. 5E, F). The pERK level at 60 min, where it usually peaks, remained at the basal level in the knockdown cells.

Hence, IGF1R acts as a functional GPCR hybrid that can interact with players in the cascade, such as ARRB1, in disease scenarios. Thus, the next step was to understand the status of cyclic AMP, which is the key output of GPCR pathways.

## cAMP Assays Suggest that IGF1R Is at the Crux of Degenerative Aβ Signaling

Here, we performed a luminescence-based assay designed for screening GPCRs in the context of an RTK, with Aβ serving as an induction agent. The cells were serum starved, after which the individual components were added to the media. The assay utilized PKA as a reagent, as it uses cAMP from lysed cells to phosphorylate its substrate via ATP. The ATP remaining after the reaction was quantified through a luciferase assay. The luminescence was inversely proportional to the cyclic AMP concentration. The raw luminescence values were used to calculate the changes in cAMP (Supplementary material S3, Fig. S4). The concentration of cAMP is presented here instead of individual fold changes to allow comparisons among different classes and to emphasize the multifactorial nature of the ARRB1 and IGF1R/INSR interaction. In the case of AD, we observed 14 more RLUs than in the control, which corresponded to a cyclic AMP accumulation of 12.60 nM over 48 h (Fig. 6A). Compared with the control, transfection with AICD decreased the RLU by 0.06-fold, indicating an insignificant change in cAMP. Aβ strongly contributed to the increase in RLUs observed in AD patients, in which the luminescence was altered by 71-fold, which resulted in a significant decrease in cAMP (0.43 nM).

To better understand the role of INSR and IGF1R, cAMP levels were measured and compared with those of the negative control Si (Fig. 6B). Moreover, IGF1R and INSR were overexpressed and assayed for cyclic AMP dysregulation (Fig. 6C). All the experiments were conducted in the presence of Aβ. Interestingly, INSR and IGF1R had varying effects on cAMP. Compared with INSR, IGF1R increased cAMP production by 0.11 nM, indicating that IGF1R positively influences cAMP accumulation. We also found a significant difference between IGF1R-overexpressing (OE) and ARRB1-knockdown cells, revealing that knocking down ARRB1 led to a decrease in cAMP. The mean cAMP output for the ARRB1-SI-treated cells was 12.06 nM, that for the IGF1R OE-treated cells was 12.88 nM, and that for the ARRB1-SI-treated cells with IGF1R OE was 12.45 nM. This clearly illustrated that the interaction between IGF1R and ARRB1 was significantly important for cAMP output.

To determine the potential for crosstalk of IGF1R, which might lead to cAMP alteration, we introduced ligands and

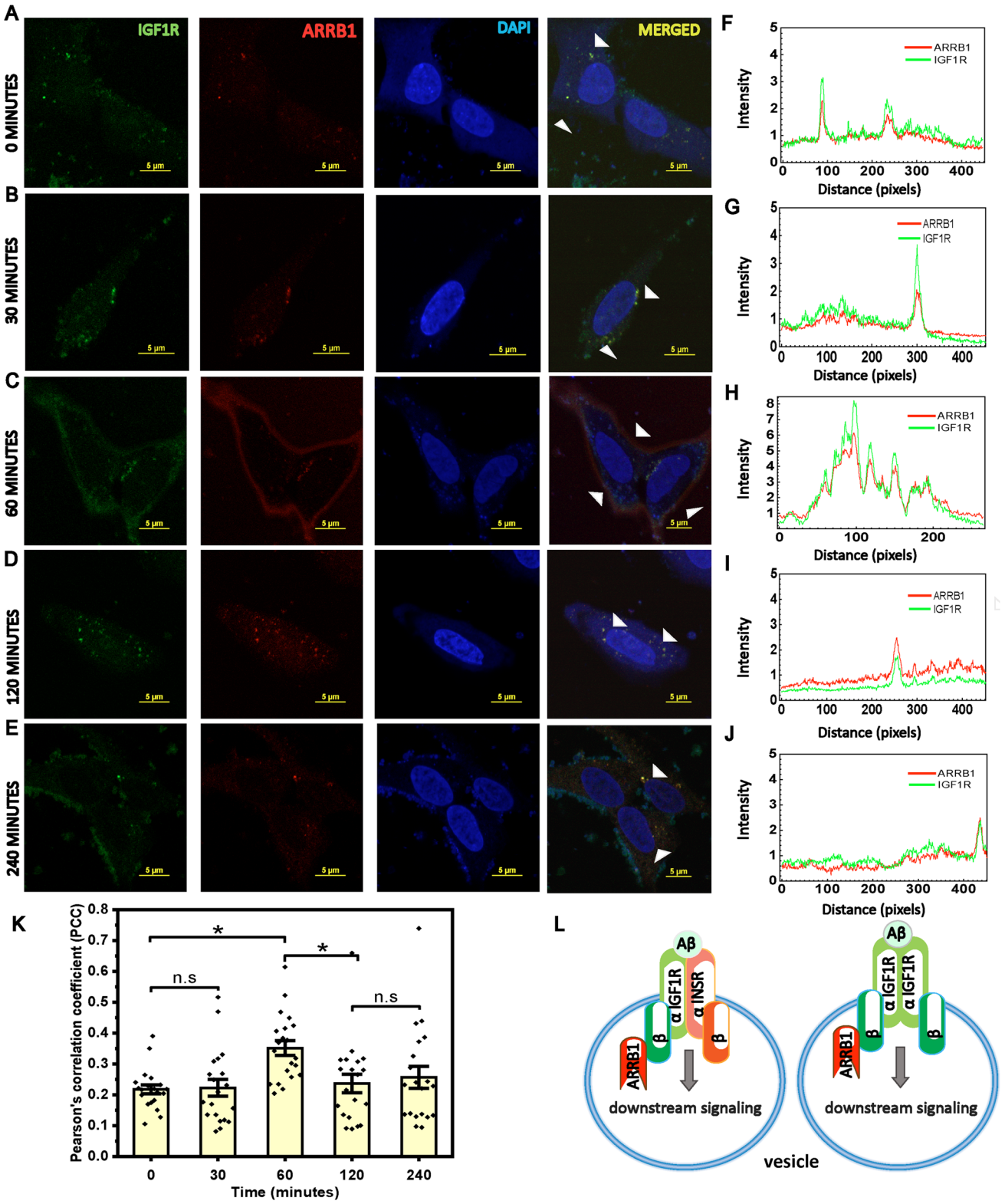


**Fig. 4** **A**–**E** show the localization of ARRB1 and IGF1R with respect to the time of treatment with Aβ. **F**–**J** show the respective plot profiles for 0, 30, 60, 120, and 240 min of treatment with Aβ. **K** Pearson's correlation coefficients for IGF1R and ARRB1 ($n = 20$). A significant change in the coefficient is denoted by *, indicating a $p$-value > 0.01 but < 0.05. Scale bar—5 µm. **L** The colocalization of HybR and/or IGF1R homodimers was analyzed

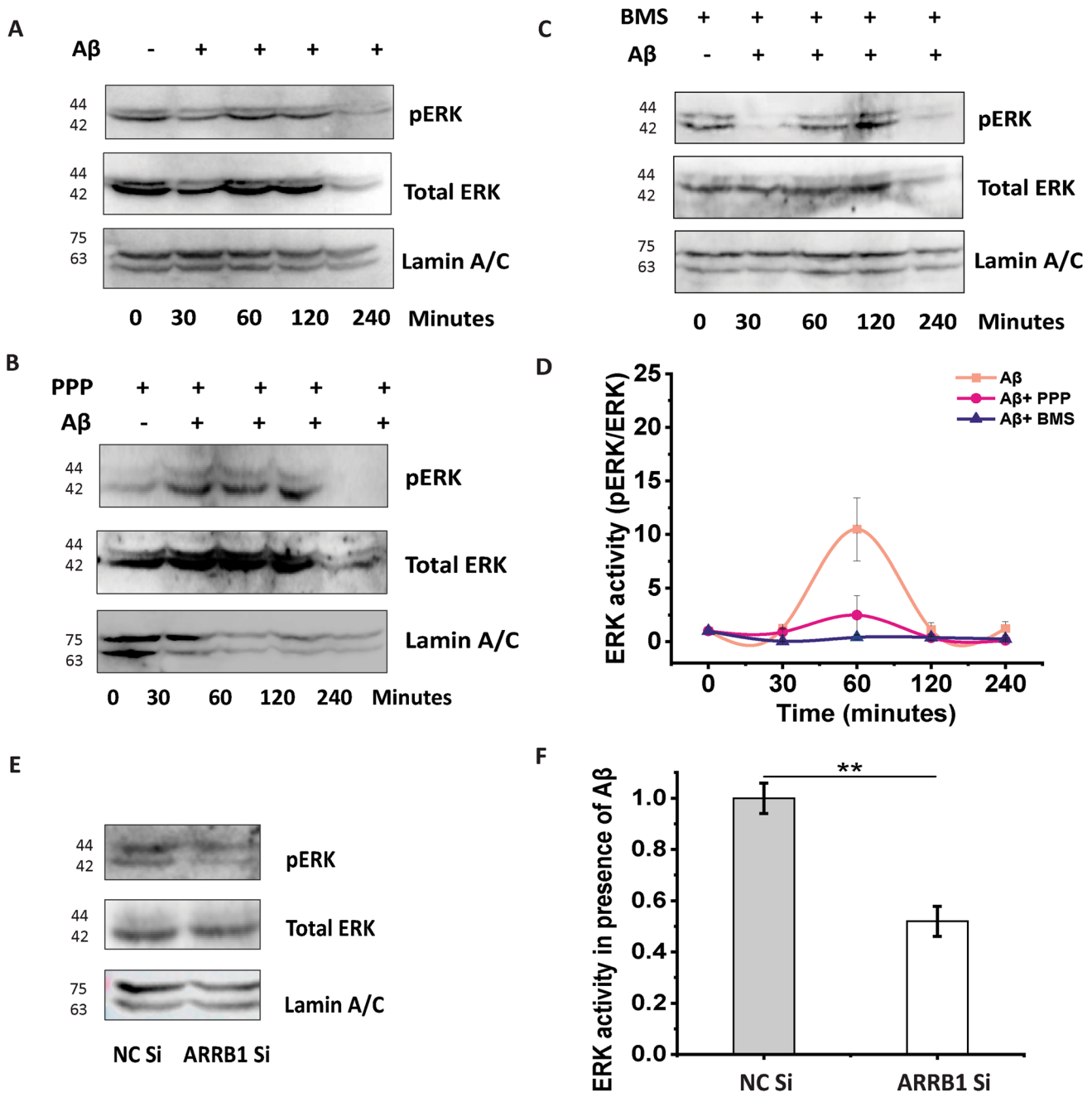


**Fig. 5** **A** Western blots showing the time course of pERK activation, along with total ERK and the loading control, Lamin A/C, in response to Aβ. **B** PPP (a selective blocker of IGF1R activity) was added 30 min prior to Aβ stimulation for different durations, after which the pERK and total ERK levels, as well as those of the loading control, were measured. **C** Effects of INSR and the IGF1R (dual inhibitor) BMS on pERK activation in the presence of Aβ over a 240-min period. **D** Relative pERK activity plotted against time, showing alterations in activity with respect to the treatments. All the experiments were conducted in triplicate. **E** To evaluate whether this activation is the result of IGF1R interacting with ARRB1 and not just canonical RTK signaling, IGF1R-overexpressing SHSY5Y cells were treated with ARRB1 siRNA or NC siRNA and subjected to Aβ treatment. The cells were then harvested and immunoblotted. **F** The relative activity of pERK when ARRB1 was knocked down at 60 min. The experiments were performed in triplicate, error bars indicate ± SEM, and the significance between pairs is represented by stars (***$p < 0.001$)

blockers of conventional pathways (Fig. 6D). Individual canonical ligands, IGF1 and Ins, were introduced in the presence or absence of Aβ to compare the relative differences between the canonical pathways and to understand the differences in the abundance of Aβ, such as in disease scenarios. IGF1 and Aβ had similar effects on cAMP, and the

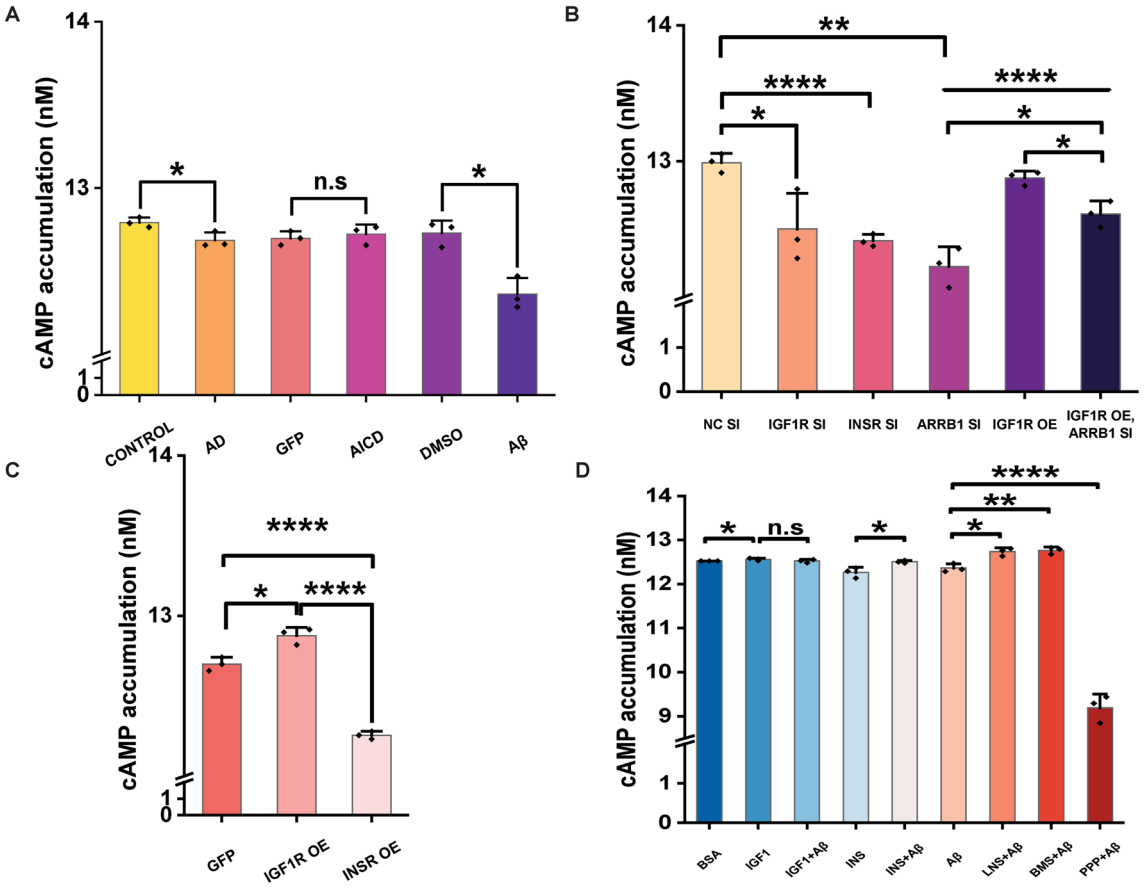


**Fig. 6** **A** SHSY5Y cells were transfected with AICD or Aβ together as in the case of AD or independently and compared with their respective controls. **B** The impact of sequentially and simultaneously knocking down the receptors and ARRB1 on cAMP in the presence of Aβ is shown. **C** The corresponding cAMP outputs for the overexpression of the receptors are shown. **D** The cAMP concentrations of IGF1R/INSR inhibitors, such as linsitinib (Lns), BMS-754807, and the IGF1R-specific inhibitor (PPP), along with ligands, Ins, and IGF1, are shown along with their respective controls. Their significance is illustrated and compared with that of Aβ and/or the control (error bars indicate ± SEM, and significant differences between pairs are represented by asterisks (*$p<0.05$; **$p<0.01$, ***$p<0.001$, ****$p<0.0001$)). The concentration of cAMP has been compared among different classes, and the findings emphasize the multifactorial nature of the ARRB1 and IGF1R/INSR interaction

difference in yield was thus nonsignificant. However, insulin and Aβ together increased cAMP production further than insulin alone did. The distinct role of the insulin receptor family (IGF1R and INSR) in cAMP upregulation is important. Inhibition of kinase activity through linsitinib (Lns) and BMS-754807 (inhibitors of the insulin receptor family with varied affinities) increased cAMP output. This finding was counterintuitive; however, the mechanism of inhibition of IGF1R is better understood than that of picropodophyllin (PPP), which selectively inhibits IGF1R. Lns and BMS are ATP competitive inhibitors that block the phosphorylation of the cytosolic tail. However, the PPP, an ATP-independent selective inhibitor of IGF1R, inhibits the receptor by interfering with the action of ARRB1. The PPP did not compete with IGF1R but downregulated and degraded the receptor, leading to a significant decrease in cAMP output compared with that in Aβ-treated cells.

These findings indicated that the cAMP dysregulation observed in response to Aβ was an outcome of the interaction between IGF1R and ARRB1, which contributed significantly to the pool. cAMP outputs constantly increased in the presence of IGF1R and ARRB1 and were significantly reduced in the absence of this interaction, as validated through siRNA- and inhibitor-based experiments. To understand whether this interaction also involves the Akt pathway, we validated the activity of Akt in the presence of Aβ and the PPP along with Aβ (Fig. S5). We found a positive correlation in terms of the effect of the PPP on Akt phosphorylation; however, the precise mechanism through which this occurs is unknown. This is nevertheless a positive indication [47], as studies have shown that enhancing Akt activity can enhance cognition in memory-impaired individuals [69, 70].

To understand the impact of the ligands and inhibitors on the fate of cells, a cell viability assay was conducted in

the presence of Aβ. Cell viability improved markedly in the presence of linsitinib to approximately $12\times10^3$ from $2\times10^3$, as observed in the presence of only Aβ (Fig. 7A). However, the best outcome was observed for the PPP, which selectively blocks IGF1R activity. The PPP blocks the interaction of IGF1R with ARRB1; thus, cell viability is improved through the inhibition of both hybrid signaling and homodimer signaling through IGF1R. Knocking down INSR and IGF1R individually led to a decrease in cell viability, indicating that they positively impact cellular health when expressed in regulated quantities (Fig. 7B). ARRB1, however, does not directly impact cellular health unless it is associated with other partners. Individual ligands, such as insulin and IGF1, did not decrease viability but did increase survival in the presence of Aβ (Fig. 7C). Together, the overexpression of ARRB1 and IGF1R observed in Alzheimer's disease has detrimental effects on cell viability (Fig. 7D). IGF1R overexpression alone can significantly improve viability; however, overexpression of ARRB1 decreases viability, which clearly shows that biased signaling through IGF1R in the presence of Aβ contributes to the decrease in cell viability observed in this disease scenario. These results, together with those of signaling studies, show that biased signaling through IGF1R via ARRB1 association contributes to the detrimental effect of Aβ on cell viability.

## Discussion

This study particularly attempts to determine the less characterized and poorly understood pathways of IGF1R in AD. Although substantial work has been done on the ligands involved, the promiscuity of the receptors and the influence of Aβ aggregation have convoluted the detailed mechanistic understanding of these pathways. Owing to their inherent structural similarities, the two receptors, IGF1R and INSR, are difficult to study individually in disease scenarios, increasing complexity further. Here, we attempt to employ a reductionist approach and pin the key players in signaling. Metascape analysis revealed that the proteins IGF1R, INSR, ARRB1, and ARRB2 could functionally form a PPI, and all four members were involved in the MAPK pathway, the

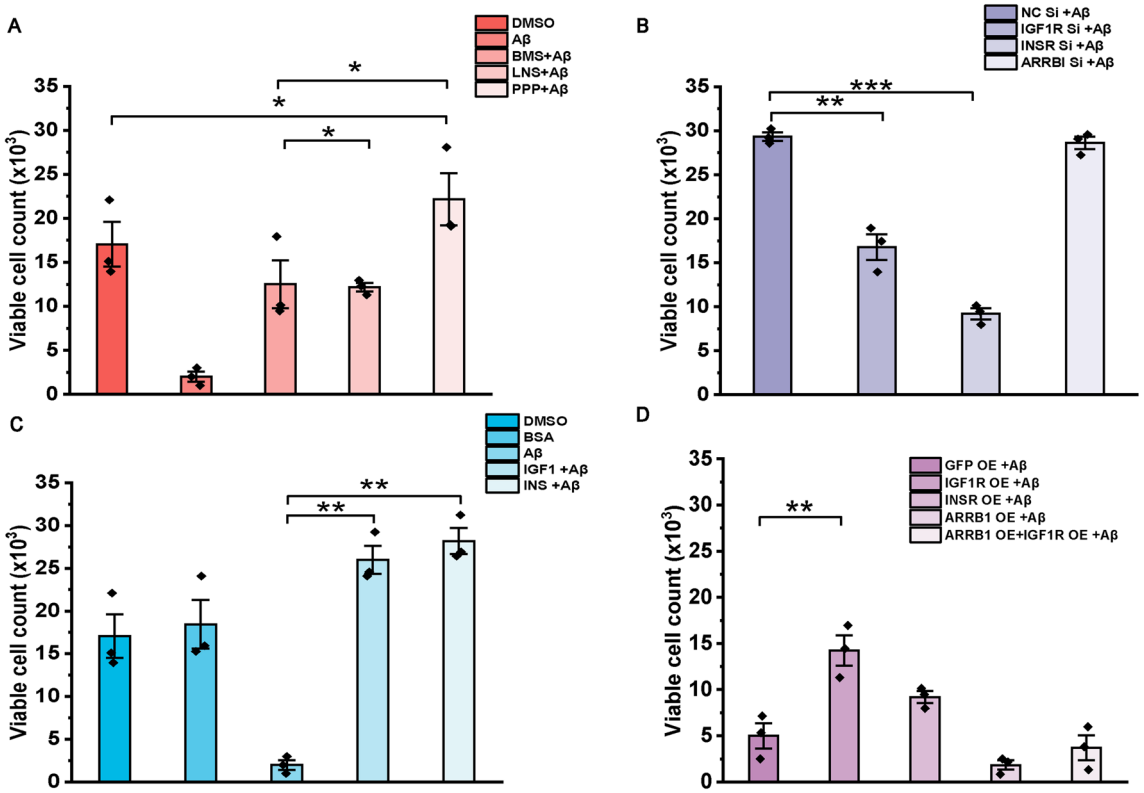


**Fig. 7** **A** SHSY5Y cells were transfected with Aβ alone or in combination with the inhibitors linsitinib (Lns), BMS-754807, and an IGF1R-specific inhibitor (PPP) to validate the impact of signaling on cell viability. **B** Cell viability was altered upon knocking down IGF1R, INSR, or ARRB1 in the presence of Aβ. **C** Effects of ligands, including both insulin (Ins) and insulin-like growth factor 1 (IGF1), on cell viability in the presence of Aβ in terms of cell viability. **D** The overexpression of receptors, including IGF1R and INSR, significantly changed cell viability. The overexpression of ARRB1, however, has a detrimental effect on cell viability in the disease landscape. The error bars indicate the ± SEMs, and the significance between pairs is represented by asterisks (*$p<0.05$; **$p<0.01$, ***$p<0.001$)

mechanism of which is unexplored from a neurodegenerative perspective.

We observed elevated IGF1R and INSR expression in our AD-like cell model. The expression of ARRB1 also increased. The propensity to form functionally active hybrids was also found to increase in response to Aβ, indicating that Aβ activates the hybrid receptor in AD. These findings indicate the presence of functional receptor hybrids, in which INSR binds to Aβ, and downstream signaling through ARRB1-mediated ERK and cAMP alterations is orchestrated by IGF1R. The formation of hybrid receptors (HybRs) of IGF1R/INSR has been documented and analyzed previously [19–21] but not in a neurodegenerative context. Their structures have been characterized recently, and they are of utmost importance for developing a thorough understanding of these receptors.

The recruitment of ARRB1 and ARRB2 to IGF1R has been previously described [31, 71–73]. The binding of ARRB1 and 2 to IGF1R controls ubiquitination and desensitization [74]. In contrast, ARRB2 forms a complex with Akt, Src, and the insulin receptor (InsR) [74, 75]. Most of these studies focused on the IGF1R/InsR axis; however, they were performed in cancer or diabetic models [32]. There is currently a gap in understanding the underlying mechanism in the case of AD, as there is no fundamental consensus on β-arrestin expression or mechanism of action in the few studies that have focused on adaptors [68, 76, 77]. However, β-arrestins bind to activated receptors and subsequently differentially regulate signaling cascades [31, 74, 78]. Seminal studies from the Lefkowitz group revealed that ARRB1 can bind to IGF1R and promote clathrin-mediated endocytosis, ERK signaling, and DNA synthesis, as in the case of GPCRs [78–81]. IGF1R is a critical receptor that participates in several signaling pathways; thus, it is important to recognize these parallel processes together to develop a holistic understanding of this process, especially in multifactorial diseases such as Alzheimer's disease.

Since ARRB1, along with IGF1R, is elevated under AD-like conditions, we performed confocal microscopy on cells overexpressing IGF1R and ARRB1, which were fixed at different times after Aβ treatment for 240 min. Notably, there was increased colocalization of ARRB1 and IGF1R 60 min after Aβ treatment. The receptors line the membrane along with ARRB1, as represented by the intensity plots, and there was a significant increase in colocalization (PCC-0.35) compared with that at 0 min of Aβ. This finding shows that Aβ in real-time triggers the recruitment of ARRB1 at approximately 60 min. The coefficients also indicate that the association reaches a maximum at 1 h and then tapers down. Previous work has shown that the recruitment of arrestin [82, 83] allows for ERK signaling, whereas in endosomes, this response to Aβ might allow for endosomal ERK signaling. However, this study is limited by the transfection efficiency, which led to a relatively low PCC. The DNA load had to be stringently controlled, as transfection with higher quantities of plasmid DNA overexpressing, ARRB1, and IGF1R proved to be cytotoxic (data not shown).

Since we observed vesicles that appeared as "puncta" when imaging the association between IGF1R and ARRB1, we investigated the pERK status in response to Aβ stimulation. We found that peak signal transduction through the ERK pathway (MAPK pathway) occurred at 60 min. Imaging studies corroborated well with the Western blot results, indicating that the association of ARRB1 and IGF1R at the membrane possibly contributes to ERK. ARRB1 was knocked down in IGF1R-overexpressing cells, and a two-fold decrease was detected, confirming that the ARRB1 interaction contributes to the increased pERK activity induced by Aβ. We further showed that the PPP, an inhibitor specific for IGF1R, can reduce pERK levels 3.25-fold compared with 13.44-fold (observed for only Aβ at 1 h). Inhibition of BMS (a dual inhibitor of IGF1R and INSR) reduced the pERK signal to a minimum of 0.54, indicating that the upregulation of the ERK cascade is mainly due to the upregulation of IGF1R and INSR in the presence of Aβ. In this respect, a few concepts are key to understanding these cascades.

Importantly, both the PPP and BMS act as inhibitors of INSR/IGF1R activation. PPP specifically inhibits IGF1R, and BMS inhibits both. We fundamentally wanted to verify whether one is more effective than the other in the presence of Aβ for the inhibition of the activity of the MAPK pathway. The assumption was that if the ERK pathway operates via INSR/IGF1R, BMS would be more effective in normalizing the activity to basal levels, which is what we observed. The comparisons were made with 0 min of treatment data for each intervention since the activity was observed to be time-dependent in the presence of only Aβ. The data showing differences in the activity of ERK after 1 h of Aβ, PPP, and BMS treatment are shown in Fig. 5D.

Ligands determine the choice of signaling cascade through the evolution of biased ligands, and particular ligands play a deterministic role in a downstream cascade [84, 85]. Another important concept to understand is the idea of signaling waves [86]. The current paradigm suggests a three-wave hypothesis for cAMP signaling by GPCRs, in which the receptor canonically binds to agonists and a change in structural conformation leads to the initiation of signaling, where cAMP is produced via Gαs GTP signaling (first wave). The receptors are subsequently endocytosed, and endosomal signaling leads to an increase in ERK signaling (second wave). Finally, $Ca^{2+}$ (an effector) enters the nucleus and activates soluble adenylate cyclase (sAC), which leads to cyclic AMP generation that upregulates PKA and transcription factors (third wave) [86, 87]. We thus focused

on cyclic AMP (cAMP) alterations downstream to track the extent and nature of the functional relationship in AD to determine the complex underlying mechanism of pathological amyloidogenesis.

To the best of our knowledge, the ability of RTKs to functionally regulate cyclic AMP has only once been shown [88]. Here, we performed a thorough analysis of cAMP accumulation in response to IGF1R and INSR overexpression, ligand stimulation, knockdown, and inhibitors to determine the connection between these two factors and Aβ abundance. We observed that the PPP, which disrupts the interaction of ARRB1 with IGF1R through its ATP noncompetitive mechanism, decreased cAMP accumulation. This finding further illustrates that the binding of ARRB1 is crucial for cAMP control. This binding of ARRB1 to IGF1R decreases cell viability. The upregulation of individual receptors contributes positively to survival and viability, and ligands participate in a positive signaling cascade when introduced along with Aβ. However, the biased nature of Aβ-mediated signaling directs the cell toward sustained cascades in the absence of original ligands (as observed in aging individuals [89, 90]), which markedly reduces cell viability in AD. Furthermore, it is important to mention here that studies have shown that cAMP increases Aβ production [91] and thus might contribute to the cell death observed in this study. The antagonism between cAMP and ERK has been reported previously [92]; however, we found that the PPP can successfully block both in disease conditions while maintaining cell viability, which is a major step toward alleviating AD.

Thus, we elucidated a novel pathway through which Aβ can influence cAMP and ERK levels. With respect to IGF1R, its abrogation has been previously shown to alleviate AD [13]; however, since β-arrestin and cAMP are usually gauged for GPCR-mediated signaling, the connection of this phenomenon to IGF1R signaling has remained elusive in AD. However, more studies are needed to explore the relationships between these proteins in detail, including their interactions with other complexes, to fully comprehend the extent of their involvement in the disease.

## Conclusion

Insulin signaling defects have long been studied in the context of dementia. However, IGF1R signaling has remained quite elusive throughout the literature, with contrasting studies and inconclusive trials [93, 94]. This study focused on the unique role of ARRB1-mediated signaling through IGF1R and downstream ERK and cAMP dysregulation in a neurodegenerative context for the first time. Conventional RTK pathways have been studied in the past, but the potential of using IGF1R and INSR as hybrids has recently been revealed; hence, signaling related to AD is unknown, which is another novel facet of this study. We discovered that beta-arrestin1 is upregulated in Alzheimer's disease and binds to IGF1R in the presence of Aβ. The hybrid formed by the conjunction of these two receptors is also altered in the presence of Aβ. The colocalization of Aβ was greatest at 60 min, after which it gradually decreased for 240 min. Interactions between IGF1R and β-arrestins have been shown several times but not in neurodegenerative conditions. This interaction has an effect on ERK and cAMP signaling. The pERK profiles for Aβ corroborated the imaging data and presented maximal values at the same time points. This interaction also leads to alterations in cyclic AMP levels. The alteration in cAMP is caused mainly by a site specific to IGF1R, which is blocked by the PPP but not by the other two inhibitors, or BMS. The greater active population of phosphorylated IGF1R found in the case of AD is noteworthy, and the downstream signaling pathways activated through hybrids in AD lead to a reduction in cell viability. However, in the current context of cAMP and ERK alterations, these individual receptors and their heterodimers likely play a determining role, opening up therapeutic possibilities for PPPs and analogs to target these receptors in the future.

**Supplementary Information** The online version contains supplementary material available at https://doi.org/10.1007/s12035-025-04735-6.

**Acknowledgements** We wish to thank Dr. M. Mahendar, SINP, Kolkata for his assistance with confocal microscopy. P.S. thanks Department of Atomic Energy for her fellowship.

**Author Contribution** P.S: Writing – original draft, Writing – review & editing, Visualization, Software, Investigation, Formal analysis, Data curation, Conceptualization. D.M: Writing – review & editing, supervision, project administration, funding acquisition, and data conceptualization.

**Funding** Open access funding provided by Department of Atomic Energy. This work was supported by the Department of Atomic Energy, GoI, RSI4002.

**Data Availability** Data supporting the findings of this study are available within the paper and supplementary. The raw data supporting this study's findings are available from the corresponding author upon reasonable request.

## Declarations

**Ethics Approval and Consent to Participate** Not applicable.

**Consent for Publication** Not applicable.

**Competing Interests** The authors declare no competing interests.

## References


1. Mathys H, Peng Z, Boix CA, Victor MB, Leary N, Babu S, Abdelhady G, Jiang X et al (2023) Single-cell atlas reveals correlates of high cognitive function, dementia, and resilience to Alzheimer's disease pathology. Cell 186:4365-4385.e27. https://doi.org/10.1016/j.cell.2023.08.039
2. Srivastava S, Ahmad R, Khare SK (2021) Alzheimer's disease and its treatment by different approaches: a review. Eur J Med Chem 216:113320. https://doi.org/10.1016/j.ejmech.2021.113320
3. Abeysinghe AADT, Deshapriya RDUS, Udawatte C (2020) Alzheimer's disease; a review of the pathophysiological basis and therapeutic interventions. Life Sci 256:117996. https://doi.org/10.1016/j.lfs.2020.117996
4. Schiöth HB, Craft S, Brooks SJ, Frey WH, Benedict C (2012) Brain insulin signaling and Alzheimer's disease: current evidence and future directions. Mol Neurobiol 46:4–10. https://doi.org/10.1007/s12035-011-8229-6
5. Sengupta P, Mukhopadhyay D (2021) Possibilities of combinatorial therapy: insulin dysregulation and the growth hormone perspective on neurodegeneration, IntechOpen https://doi.org/10.5772/intechopen.97002.
6. Heldin C-H, Lennartsson J (2016) Receptor tyrosine kinases and their ligands, in: R.A. Bradshaw, P.D. Stahl (Eds.), Encyclopedia of Cell Biology, Academic Press, Waltham, pp. 8–21. https://doi.org/10.1016/B978-0-12-394447-4.30001-3.
7. Sengupta P, Das R, Majumder P, Mukhopadhyay D (2024) Connecting the ends: signaling via receptor tyrosine kinases and cytoskeletal degradation in neurodegeneration. Explor Neurosci. 3:1–26. https://doi.org/10.37349/en.2024.00033
8. da Costa IB, de Labio RW, Rasmussen LT, Viani GA, Chen E, Villares J, Payao SL (2017) Change in INSR, APBA2 and IDE gene expressions in brains of Alzheimer's disease patients. Curr Alzheimer Res 14(7):760–765. https://doi.org/10.2174/1567205014666170203100734
9. Kellar D, Craft S (2020) Brain insulin resistance in Alzheimer's disease and related disorders: mechanisms and therapeutic approaches. The Lancet Neurology 19:758–766. https://doi.org/10.1016/S1474-4422(20)30231-3
10. Leclerc M, Bourassa P, Tremblay C, Caron V, Sugère C, Emond V, Bennett DA, Calon F (2023) Cerebrovascular insulin receptors are defective in Alzheimer's disease. Brain 146:75–90. https://doi.org/10.1093/brain/awac309
11. Hallschmid M (2021) Intranasal insulin for Alzheimer's disease. CNS Drugs 35:21–37. https://doi.org/10.1007/s40263-020-00781-x
12. Sengupta P, Sen S, Mukhopadhyay D (2024) The receptor tyrosine kinase IGF1R and its associated GPCRs are co-regulated by the noncoding RNA NEAT1 in Alzheimer's disease. Gene 918:148503. https://doi.org/10.1016/j.gene.2024.148503
13. Park JY, Darvas M, Ladiges W (2022) Targeting IGF1R signaling for brain aging and Alzheimer's disease. Aging Pathobiol Ther 4:129–131. https://doi.org/10.31491/apt.2022.12.103
14. Boucher J, Tseng Y-H, Kahn CR (2010) Insulin and insulin-like growth factor-1 receptors act as ligand-specific amplitude modulators of a common pathway regulating gene transcription. J Biol Chem 285:17235–17245. https://doi.org/10.1074/jbc.M110.118620
15. Hupfeld CJ, Olefsky JM (2007) Regulation of receptor tyrosine kinase signaling by GRKs and β-arrestins. Annu Rev Physiol 69:561–577. https://doi.org/10.1146/annurev.physiol.69.022405.154626
16. Girnita L, Worrall C, Takahashi S-I, Seregard S, Girnita A (2014) Something old, something new and something borrowed: emerging paradigm of insulin-like growth factor type 1 receptor (IGF-1R) signaling regulation. Cell Mol Life Sci 71:2403–2427. https://doi.org/10.1007/s00018-013-1514-y
17. Maharana J, Banerjee R, Yadav MK, Sarma P, Shukla AK (2022) Emerging structural insights into GPCR–β-arrestin interaction and functional outcomes. Curr Opin Struct Biol 75:102406. https://doi.org/10.1016/j.sbi.2022.102406
18. George C, Gontier G, Lacube P, François J-C, Holzenberger M, Aïd S (2017) The Alzheimer's disease transcriptome mimics the neuroprotective signature of IGF-1 receptor-deficient neurons. Brain 140:2012–2027. https://doi.org/10.1093/brain/awx132
19. Xu Y, Margetts MB, Venugopal H, Menting JG, Kirk NS, Croll TI, Delaine C, Forbes BE et al (2022) How insulin-like growth factor I binds to a hybrid insulin receptor type 1 insulin-like growth factor receptor. Structure 30:1098-1108.e6. https://doi.org/10.1016/j.str.2022.05.007
20. Turvey SJ, McPhillie MJ, Kearney MT, Muench SP, Simmons KJ, Fishwick CWG (2022) Recent developments in the structural characterisation of the IR and IGF1R: implications for the design of IR–IGF1R hybrid receptor modulators. RSC Med Chem 13:360–374. https://doi.org/10.1039/d1md00300c
21. Chen J, Nagle AM, Wang Y-F, Boone DN, Lee AV (2018) Controlled dimerization of insulin-like growth factor-1 and insulin receptors reveals shared and distinct activities of holo and hybrid receptors. J Biol Chem 293:3700–3709. https://doi.org/10.1074/jbc.M117.789503
22. Kineman RD, Del Rio-Moreno M, Sarmento-Cabral A (2018) 40 years of IGF1: understanding the tissue-specific roles of IGF1/IGF1R in regulating metabolism using the Cre/loxP system. J Mol Endocrinol 61:T187–T198. https://doi.org/10.1530/JME-18-0076
23. Curtis D, Bandyopadhyay S (2021) Mini-review: role of the PI3K/Akt pathway and tyrosine phosphatases in Alzheimer's disease susceptibility. Ann Hum Genet 85:1–6. https://doi.org/10.1111/ahg.12410
24. Zhu X, Lee H, Raina AK, Perry G, Smith MA (2002) The role of mitogen-activated protein kinase pathways in Alzheimer's disease. Neurosignals 11:270–281. https://doi.org/10.1159/000067426
25. Muraleva NA, Kolosova NG, Stefanova NA (2021) MEK1/2-ERK pathway alterations as a therapeutic target in sporadic Alzheimer's disease: a study in senescence-accelerated OXYS rats. Antioxidants 10:1058. https://doi.org/10.3390/antiox10071058
26. Kim EK, Choi EJ (2010) Pathological roles of MAPK signaling pathways in human diseases. Biochimica et Biophysica Acta (BBS) - Mol Basis Dis 1802:396–405. https://doi.org/10.1016/J.BBADIS.2009.12.009
27. Morrison DK (2012) MAP kinase pathways. Cold Spring Harb Perspect Biol 4:a011254. https://doi.org/10.1101/cshperspect.a011254
28. Kirouac L, Rajic AJ, Cribbs DH, Padmanabhan J (2017) Activation of Ras-ERK signaling and GSK-3 by amyloid precursor protein and amyloid beta facilitates neurodegeneration in Alzheimer's disease. eNeuro 4(2):0ENEURO.149-16.2017. https://doi.org/10.1523/ENEURO.0149-16.2017
29. Kins S, Kurosinski P, Nitsch RM, Götz J (2003) Activation of the ERK and JNK signaling pathways caused by neuron-specific inhibition of PP2A in transgenic mice. Am J Pathol 163:833–843

30. Albert-Gascó H, Ros-Bernal F, Castillo-Gómez E, Olucha-Bordonau FE (2020) MAP/ERK signaling in developing cognitive and emotional function and its effect on pathological and neurodegenerative processes. Int J Mol Sci 21:4471. https://doi.org/10.3390/ijms21124471
31. Suleymanova N, Crudden C, Shibano T, Worrall C, Oprea I, Tica A, Calin GA, Girnita A, Girnita L (2017) Functional antagonism of β-arrestin isoforms balance IGF-1R expression and signalling with distinct cancer-related biological outcomes. Oncogene 36:5734–5744. https://doi.org/10.1038/onc.2017.179
32. Werner H, Sarfstein R, Laron Z (2021) The role of nuclear insulin and IGF1 receptors in metabolism and cancer. Biomolecules 11:531. https://doi.org/10.3390/biom11040531
33. Chen MK, Hsu JL, Hung MC (2020) Nuclear receptor tyrosine kinase transport and functions in cancer. Adv Cancer Res 147:59–107. https://doi.org/10.1016/BS.ACR.2020.04.010
34. Kesten D, Horovitz-Fried M, Brutman-Barazani T, Sampson SR (1865) Insulin-induced translocation of IR to the nucleus in insulin responsive cells requires a nuclear translocation sequence. Biochimica et Biophysica Acta (BBA) - Molecular Cell Research 2018:551–559. https://doi.org/10.1016/j.bbamcr.2018.01.004
35. Mills JV, Osher E, Rieunier G, Mills IG, Macaulay VM (2021) IGF-1R nuclear import and recruitment to chromatin involves both alpha and beta subunits. Discov Onc 12:13. https://doi.org/10.1007/s12672-021-00407-8
36. Chughtai S (2020) The nuclear translocation of insulin-like growth factor receptor and its significance in cancer cell survival. Cell Biochem Funct 38:347–351. https://doi.org/10.1002/cbf.3479
37. Sehat B, Tofigh A, Lin Y, Trocmé E, Liljedahl U, Lagergren J, Larsson O (2010) SUMOylation mediates the nuclear translocation and signaling of the IGF-1 receptor. Sci Signaling 3:10. https://doi.org/10.1126/scisignal.2000628
38. Mattsson N, Palmqvist S, Stomrud E, Vogel J, Hansson O (2019) Staging β-amyloid pathology with amyloid positron emission tomography. JAMA Neurol 76:1319–1329. https://doi.org/10.1001/jamaneurol.2019.2214
39. Chételat G, Villemagne VL, Pike KE, Ellis KA, Ames D, Masters CL, Rowe CC (2012) and the Australian Imaging Biomarkers and Lifestyle Study of Ageing (AIBL) Research Group, Relationship between memory performance and β-amyloid deposition at different stages of Alzheimer's disease. Neurodegener Dis 10:141–144. https://doi.org/10.1159/000334295
40. Zhou Y, Zhou B, Pache L, Chang M, Khodabakhshi AH, Tanaseichuk O, Benner C, Chanda SK (2019) Metascape provides a biologist-oriented resource for the analysis of systems-level datasets. Nat Commun 10:1523. https://doi.org/10.1038/s41467-019-09234-6
41. Majumder P, Roy K, Bagh S, Mukhopadhyay D (2019) Receptor tyrosine kinases (RTKs) consociate in regulatory clusters in Alzheimer's disease and type 2 diabetes. Mol Cell Biochem 459:171–182. https://doi.org/10.1007/s11010-019-03560-5
42. Piñero J, Ramírez-Anguita JM, Saüch-Pitarch J, Ronzano F, Centeno E, Sanz F, Furlong LI (2020) The DisGeNET knowledge platform for disease genomics: 2019 update. Nucleic Acids Res 48:D845–D855. https://doi.org/10.1093/nar/gkz1021
43. Bader GD, Hogue CW (2003) An automated method for finding molecular complexes in large protein interaction networks. BMC Bioinformatics 4:2. https://doi.org/10.1186/1471-2105-4-2
44. Hara MR, Kovacs JJ, Whalen EJ, Rajagopal S, Strachan RT, Grant W, Towers AJ, Williams B, Lam CM, Xiao K, Shenoy SK, Gregory SG, Ahn S, Duckett DR, Lefkowitz RJ (2011) A stress response pathway regulates DNA damage through β2-adrenoreceptors and β-arrestin-1. Nature 477:349–353. https://doi.org/10.1038/nature10368
45. Pietraszewska-Bogiel A, Joosen L, Chertkova AO, Goedhart J (2020) Not so dry after all: DRY mutants of the AT1A receptor and H1 receptor can induce G-protein-dependent signaling. ACS Omega 5:2648–2659. https://doi.org/10.1021/acsomega.9b03146
46. Chanda K, Jana NR, Mukhopadhyay D (2022) Long non-coding RNA MALAT1 protects against Aβ1-42 induced toxicity by regulating the expression of receptor tyrosine kinase EPHA2 via quenching miR-200a/26a/26b in Alzheimer's disease. Life Sci 302:120652. https://doi.org/10.1016/j.lfs.2022.120652
47. Majumder P, Roy K, Singh BK, Jana NR, Mukhopadhyay D (2017) Cellular levels of Grb2 and cytoskeleton stability are correlated in a neurodegenerative scenario. Dis Models Mechanisms 10(5):655–669. https://doi.org/10.1242/dmm.027748
48. Hellstrand E, Boland B, Walsh DM, Linse S (2010) Amyloid β-protein aggregation produces highly reproducible kinetic data and occurs by a two-phase process. ACS Chem Neurosci 1:13–18. https://doi.org/10.1021/cn900015v
49. Harper JD, Lansbury PT (1997) Models of amyloid seeding in Alzheimer's disease and scrapie: mechanistic truths and physiological consequences of the time-dependent solubility of amyloid proteins. Annu Rev Biochem 66:385–407. https://doi.org/10.1146/annurev.biochem.66.1.385
50. Roberts CJ (2007) Non-native protein aggregation kinetics. Biotechnol Bioeng 98:927–938. https://doi.org/10.1002/bit.21627
51. Novo M, Freire S, Al-Soufi W (2018) Critical aggregation concentration for the formation of early amyloid-β (1–42) oligomers. Sci Rep 8:1783. https://doi.org/10.1038/s41598-018-19961-3
52. Iljina M, Garcia GA, Dear AJ, Flint J, Narayan P, Michaels TCT, Dobson CM, Frenkel D, Knowles TPJ, Klenerman D (2016) Quantitative analysis of co-oligomer formation by amyloid-beta peptide isoforms. Sci Rep 6:28658. https://doi.org/10.1038/srep28658
53. Slaaby R (2015) Specific insulin/IGF1 hybrid receptor activation assay reveals IGF1 as a more potent ligand than insulin. Sci Rep 5:7911. https://doi.org/10.1038/srep07911
54. Strömberg T, Ekman S, Girnita L, Dimberg LY, Larsson O, Axelson M, Lennartsson J, Hellman U, Carlson K, Österborg A, Vanderkerken K, Nilsson K, Jernberg-Wiklund H (2006) IGF-1 receptor tyrosine kinase inhibition by the cyclolignan PPP induces G2/M-phase accumulation and apoptosis in multiple myeloma cells. Blood 107:669–678. https://doi.org/10.1182/blood-2005-01-0306
55. Kurlawala Z, Dunaway R, Shah PP, Gosney JA, Siskind LJ, Ceresa BP, Beverly LJ (2017) Regulation of insulin-like growth factor receptors by Ubiquilin1. Biochem J 474:4105–4118. https://doi.org/10.1042/BCJ20170620
56. Wester L, Venneker S, Hazenoot M, Pont C, Koedoot E, Timmermans AM et al (2022) A kinase inhibitor screen reveals MEK1/2 as a novel therapeutic target to antagonize IGF1R-mediated antiestrogen resistance in ERα-positive luminal breast cancer. Biochem Pharmacol 204:115233. https://doi.org/10.1016/j.bcp.2022.115233
57. Nagao H, Cai W, Wewer Albrechtsen NJ, Steger M, Batista TM, Pan H, Dreyfuss JM, Mann M et al (2021) Distinct signaling by insulin and IGF-1 receptors and their extra-and intracellular domains. Proc Nat Acad Sci 118(17):e2019474118. https://doi.org/10.1073/pnas.2019474118
58. Stauffer W, Sheng H, Lim HN (2018) EzColocalization: an ImageJ plugin for visualizing and measuring colocalization in cells and organisms. Sci Rep 8:15764. https://doi.org/10.1038/s41598-018-33592-8
59. Schindelin J, Arganda-Carreras I, Frise E, Kaynig V, Longair M, Pietzsch T, Preibisch S, Rueden C et al (2012) Fiji: an open-source platform for biological-image analysis. Nat Methods 9:676–682. https://doi.org/10.1038/nmeth.2019
60. Saha S, Mukherjee S, Guha G, Mukhopadhyay D (2021) Dynamics of AQP4 upon exposure to seropositive patient serum before and after rituximab therapy in neuromyelitis optica: a cell-based

study. J Neuroimmunol 361:577752. https://doi.org/10.1016/j.jneuroim.2021.577752
61. Pichet Binette A, Gaiteri C, Wennström M, Kumar A, Hristovska I, Spotorno N, Hansson O et al (2024) Proteomic changes in Alzheimer's disease associated with progressive Aβ plaque and tau tangle pathologies. Nature Neurosci 27(10):1880–1891. https://doi.org/10.1038/s41593-024-01737-w
62. Higginbotham L, Ping L, Dammer EB, Duong DM, Zhou M, Gearing M, Hurst C, Glass JD et al (2020) Integrated proteomics reveals brain-based cerebrospinal fluid biomarkers in asymptomatic and symptomatic Alzheimer's disease. Sci Adv 6:eaaz9360. https://doi.org/10.1126/sciadv.aaz9360
63. Sathe G, Na CH, Renuse S, Madugundu AK, Albert M, Moghekar A, Pandey A (2019) Quantitative proteomic profiling of cerebrospinal fluid to identify candidate biomarkers for Alzheimer's disease. PROTEOMICS - Clin Appl 13:1800105. https://doi.org/10.1002/prca.201800105
64. Askenazi M, Kavanagh T, Pires G, Ueberheide B, Wisniewski T, Drummond E (2023) Compilation of reported protein changes in the brain in Alzheimer's disease. Nat Commun 14:4466. https://doi.org/10.1038/s41467-023-40208-x
65. Frölich L, Blum-Degen D, Bernstein H-G, Engelsberger S, Humrich J, Laufer S, Muschner D et al (1998) Brain insulin and insulin receptors in aging and sporadic Alzheimer's disease. J Neural Transm 105:423–438. https://doi.org/10.1007/s007020050068
66. Bossers K, Wirz KTS, Meerhoff GF, Essing AHW, van Dongen JW, Houba P, Kruse CG, Verhaagen J et al (2010) Concerted changes in transcripts in the prefrontal cortex precede neuropathology in Alzheimer's disease. Brain 133:3699–3723. https://doi.org/10.1093/brain/awq258
67. Liu X, Zhao X, Zeng X, Bossers K, Swaab DF, Zhao J, Pei G (2013) β-Arrestin1 regulates γ-secretase complex assembly and modulates amyloid-β pathology. Cell Res 23:351–365. https://doi.org/10.1038/cr.2012.167
68. Thathiah A, Horré K, Snellinx A, Vandewyer E, Huang Y, Ciesielska M, De Kloe G, Munck S et al (2013) β-arrestin 2 regulates Aβ generation and γ-secretase activity in Alzheimer's disease. Nat Med 19:43–49. https://doi.org/10.1038/nm.3023
69. Griffin RJ, Moloney A, Kelliher M, Johnston JA, Ravid R, Dockery P, O'Connor R, O'Neill C (2005) Activation of Akt/PKB, increased phosphorylation of Akt substrates and loss and altered distribution of Akt and PTEN are features of Alzheimer's disease pathology. J Neurochem 93:105–117. https://doi.org/10.1111/j.1471-4159.2004.02949.x
70. Long H-Z, Cheng Y, Zhou Z-W, Luo H-Y, Wen D-D, Gao L-C (2021) PI3K/AKT signal pathway: a target of natural products in the prevention and treatment of Alzheimer's disease and Parkinson's disease. Front Pharmacol 12:648636. https://doi.org/10.3389/fphar.2021.648636
71. Zheng H, Shen H, Oprea I, Worrall C, Stefanescu R, Girnita A, Girnita L (2012) β-Arrestin–biased agonism as the central mechanism of action for insulin-like growth factor 1 receptor–targeting antibodies in Ewing's sarcoma. Proc Natl Acad Sci 109:20620–20625. https://doi.org/10.1073/pnas.1216348110
72. Krieger CC, Place RF, Bevilacqua C, Marcus-Samuels B, Abel BS, Skarulis MC, Kahaly GJ, Neumann S et al (2016) TSH/IGF-1 receptor cross talk in Graves' ophthalmopathy pathogenesis. J Clin Endocrinol Metab 101:2340–2347. https://doi.org/10.1210/jc.2016-1315
73. van Gastel J, Hendrickx JO, Leysen H, Santos-Otte P, Luttrell LM, Martin B, Maudsley S (2018) β-Arrestin based receptor signaling paradigms: potential therapeutic targets for complex age-related disorders, Front Pharmacol 9. https://www.frontiersin.org/articles/10.3389/fphar.2018.01369 (accessed October 29, 2023).
74. Rodgers JT, Puigserver P (2009) Insulin resistance: β-arrestin development. Cell Res 19:275–276. https://doi.org/10.1038/cr.2009.22
75. Luan B, Zhao J, Wu H, Duan B, Shu G, Wang X, Li D, Jia W, Kang J, Pei G (2009) Deficiency of a β-arrestin-2 signal complex contributes to insulin resistance. Nature 457:1146–1149. https://doi.org/10.1038/nature07617
76. Jiang T, Yu JT, Tan MS, Zhu XC, Tan L (2013) β-Arrestins as Potential Therapeutic Targets for Alzheimer's Disease. Mol Neurobiol 48:812–818. https://doi.org/10.1007/s12035-013-8469-8
77. Potter P, Choi S, Jones D, Beach T (2018)Decreased Levels of Beta-Arrestin 1 in Brains of Patients with Alzheimer's Disease. The FASEB Journal 32:552.3–552.3. https://doi.org/10.1096/fasebj.2018.32.1_supplement.552.3
78. Shenoy SK, Lefkowitz RJ (2011) β-Arrestin-mediated receptor trafficking and signal transduction. Trends Pharmacol Sci 32:521–533. https://doi.org/10.1016/j.tips.2011.05.002
79. Cahill TJ, Thomsen ARB, Tarrasch JT, Plouffe B, Nguyen AH, Yang F, Huang LY, Kahsai AW et al (2017) Distinct conformations of GPCR–β-arrestin complexes mediate desensitization, signaling, and endocytosis. Proc Natl Acad Sci 114:2562–2567. https://doi.org/10.1073/pnas.1701529114
80. Shenoy SK, Lefkowitz RJ (2005) Seven-Transmembrane Receptor Signaling Through β-Arrestin, Science's STKE. https://doi.org/10.1126/stke.2005/308/cm10
81. Lin FT, Daaka Y, Lefkowitz RJ (1998) β-Arrestins Regulate Mitogenic Signaling and Clathrin-mediated Endocytosis of the Insulin-like Growth Factor I Receptor. J Biol Chem 273:31640–31643. https://doi.org/10.1074/jbc.273.48.31640
82. Worrall C, Suleymanova N, Crudden C, Trocoli Drakensjö I, Candrea E, Nedelcu D, Girnita A et al (2017) Unbalancing p53/Mdm2/IGF-1R axis by Mdm2 activation restrains the IGF-1-dependent invasive phenotype of skin melanoma. Oncogene 36(23):3274–3286. https://doi.org/10.1038/onc.2016.472
83. Girnita L, Shenoy SK, Sehat B, Vasilcanu R, Girnita A, Lefkowitz RJ, Larsson O (2005) β-Arrestin is crucial for ubiquitination and down-regulation of the insulin-like growth factor-1 receptor by acting as adaptor for the MDM2 E3 ligase*. J Biol Chem 280:24412–24419. https://doi.org/10.1074/jbc.M501129200
84. Kenakin T (2021) Biased signaling as allosteric probe dependence. Cell Signal 79:109844. https://doi.org/10.1016/j.cellsig.2020.109844
85. Trenker R, Jura N (2020) Receptor tyrosine kinase activation: from the ligand perspective. Curr Opin Cell Biol 63:174–185. https://doi.org/10.1016/j.ceb.2020.01.016
86. Pizzoni A, Zhang X, Altschuler DL (2023) From membrane to nucleus: a three-wave hypothesis of cAMP signaling. J Biol Chem 300:105497. https://doi.org/10.1016/j.jbc.2023.105497
87. Leybaert L, Sanderson MJ (2012) Intercellular Ca2+ waves: mechanisms and function. Physiol Rev 92:1359–1392. https://doi.org/10.1152/physrev.00029.2011
88. Tan CM, Kelvin DJ, Litchfield DW, Ferguson SSG, Feldman RD (2001) Tyrosine kinase-mediated serine phosphorylation of adenylyl cyclase. Biochemistry 40:1702–1709. https://doi.org/10.1021/bi0015818
89. Chang AM, Halter JB (2003) Aging and insulin secretion. Am J Physiol-Endocrinol Metabolism 284:E7–E12. https://doi.org/10.1152/ajpendo.00366.2002
90. Toth L, Czigler A, Hegedus E, Komaromy H, Amrein K, Czeiter E, Yabluchanskiy A, Koller A et al (2022) Age-related decline in circulating IGF-1 associates with impaired neurovascular coupling responses in older adults. GeroScience 44:2771–2783. https://doi.org/10.1007/s11357-022-00623-2
91. Ricciarelli R, Fedele E (2018) cAMP, cGMP and amyloid β: three ideal partners for memory formation. Trends Neurosci 41:255–266. https://doi.org/10.1016/j.tins.2018.02.001
92. Cui ZG, Hong N-Y, Guan J, Kang H-K, Lee D-H, Lee Y-K, Park D-B (2011) cAMP antagonizes ERK-dependent antiapoptotic

action of insulin. BMB Rep 44:205–210. https://doi.org/10.5483/BMBRep.2011.44.3.205
93. Jentzsch V, Osipenko L, Scannell JW, Hickman JA (2023) Costs and causes of oncology drug attrition with the example of insulin-like growth factor-1 receptor inhibitors. JAMA Netw Open 6:e2324977. https://doi.org/10.1001/jamanetworkopen.2023.24977
94. Soni UK, Jenny L, Hegde RS (2023) IGF-1R targeting in cancer – does sub-cellular localization matter? J Exp Clin Cancer Res 42:273. https://doi.org/10.1186/s13046-023-02850-7